

considerable variation in optical-model parameters can be found.

It is rewarding that the curve of minimum χ^2 as a function of normalization showed well-defined minima within the experimental normalization for all three angular distributions. However, because of the gross simplification of the optical-model potential as it applies to deuteron scattering, it is not obvious that the minimum *should* be at the exact normalization of the data. Consequently, it is difficult to attach much significance

to optical-model analysis solely on the basis of relative elastic-scattering cross sections. It is possible that some of the great variations in optical-model parameters found previously¹ were due to the extreme sensitivity of the parameters to the absolute normalization of the data.

ACKNOWLEDGMENTS

We take great pleasure in acknowledging the valuable assistance of R. J. Silva, G. R. Satchler, and G. F. Wells.

Elastic Scattering of Low-Energy Deuterons from ⁶⁰Ni and ¹¹⁴Cd and the Effect of the Deuteron Electric Polarizability in the Optical-Model Potential*

J. K. DICKENS AND F. G. PEREY

Oak Ridge National Laboratory, Oak Ridge, Tennessee

(Received 20 January 1965)

Differential cross sections for elastic scattering of deuterons from ⁶⁰Ni and ¹¹⁴Cd were measured for deuteron bombarding energies between 5 and 15 MeV. The data were analyzed by means of an optical model that includes a potential due to the deuteron electric polarizability. We conclude that the effects of the polarizability are small, although not negligible, and that nuclear interactions still dominate the elastic scattering at these energies.

I. INTRODUCTION

ANGULAR distributions of deuterons elastically scattered from nuclei at bombarding energies of greater than 10 MeV exhibit unmistakable diffraction patterns and can be analyzed by an optical-model potential. In a recent systematic analysis,¹ good agreement with the experimental data was obtained by use of a complex optical-model potential whose parameters vary smoothly as functions of mass number and energy. The addition of a spin-orbit potential,² similar to that used for nucleon-nucleus scattering, has given very good agreement with the measured³ vector and tensor polarization in deuteron elastic scattering and has improved the fit to the elastic-scattering angular distributions at higher energies.⁴

In all the previously mentioned analyses, the incident deuteron energy was greater than the Coulomb barrier. Also, the fact that the deuteron is a loosely bound system of a neutron and proton was ignored, and instead it was considered to be a charged nucleus at a point. Since optical-model analyses consistently reproduce experimental data, this approximation may not be a serious limitation. Thus, when the incident energy is above the Coulomb barrier, the elastic scattering of

deuterons is probably dominated by nuclear breakup of the deuterons as they penetrate the target nucleus. The imaginary part of the optical potential may reproduce the main feature of the reaction mechanism by causing strong absorption at the surface of the nucleus. However, when the deuteron energy is close to or less than the Coulomb barrier, the nuclear breakup, represented by the imaginary part of the optical-model potential, may not be the dominant mechanism, and the optical model may be unable to give a good description of the elastic scattering of deuterons.

In the earliest attempts at explaining the departure from Rutherford scattering in deuteron elastic scattering, all nuclear interactions were neglected. Consideration was given only to the fact that the center of charge of the deuteron does not always coincide with its center of mass, and that this noncoincidence will lead to an electric polarizability⁵ of the deuteron. Later, the possibility of electric breakup of the deuteron was also included.⁶ Recently, Clement⁷ calculated the effect of the nuclear electric field on the scattering of deuterons and found the effect to be so large as to make the use of nuclear optical models for deuteron scattering a doubtful procedure.

To investigate what happens to the nuclear optical-model potential as the deuteron energy approaches the

* Research sponsored by the U. S. Atomic Energy Commission under contract with the Union Carbide Corporation.

¹ C. M. Perey and F. G. Perey, *Phys. Rev.* **132**, 755 (1963).

² J. Raynal, *Phys. Letters* **7**, 281 (1963).

³ R. Beurtey *et al.*, *Compt. Rend.* **256**, 922 (1963); **257**, 1477 (1963).

⁴ C. M. Perey and F. G. Perey (to be published).

⁵ J. B. French and M. L. Goldberger, *Phys. Rev.* **87**, 899 (1952).

⁶ Y. Nishida, *Progr. Theoret. Phys. (Kyoto)* **17**, 506 (1957); **19**, 389 (1958).

⁷ C. F. Clement, *Phys. Rev.* **128**, 2728 (1962).

Coulomb barrier, we measured elastic angular distributions of deuterons, scattered from ^{60}Ni at nine energies, beginning at 5 MeV, and from ^{114}Cd at eight energies, beginning at 8 MeV. The measurements are described in the next section, and the analysis of these data in terms of a standard optical model is presented in Sec. III. The effects of the deuteron electric polarizability in the optical-model potential are discussed in Sec. IV. We conclude that nuclear interactions are dominant for $E_d \leq$ the Coulomb barrier.

II. EXPERIMENTAL DATA

The deuteron beam of the ORNL tandem Van de Graaff was scattered from self-supporting isotopically enriched ($>99\%$) foils of ^{60}Ni and ^{114}Cd that were $\sim 1 \text{ mg/cm}^2$ thick. The detector was a solid-state surface barrier counter, and the over-all resolution at the higher energies was about 50 keV (full width at half-maximum). At lower energies the resolution was limited by the energy loss in the targets. The scattering chamber and the associated electronics are described elsewhere.⁸ For both targets excitation functions were obtained over

the complete energy range, taking data points every 250 keV, for $\theta_{\text{lab}} = 60$ and 110° . No structure was observed in any of these excitation curves.

Statistical errors in the numbers of counts in the elastic peaks were negligible. The error in the subtraction of the proton background [due to (d,p) reactions] is estimated to be $<1\%$. Since these errors are small, an estimate of the error in the relative cross section was obtained from the reproducibility of the data points. In all cases tried the error in the reproduction was less than 3%. The absolute error assigned to the measured cross sections depended primarily on the measured target thicknesses, the detector solid-angle measurement, and the beam integration measurements, and was estimated to be better than 10%. From the excitation curves the relative cross sections at the different energies are estimated to be good to $\pm 5\%$. The data⁹ are shown in Fig. 1 with the best optical-model fits obtained.

III. OPTICAL-MODEL ANALYSIS

The standard optical model used is the same as that described in an earlier article.¹ The nuclear potential

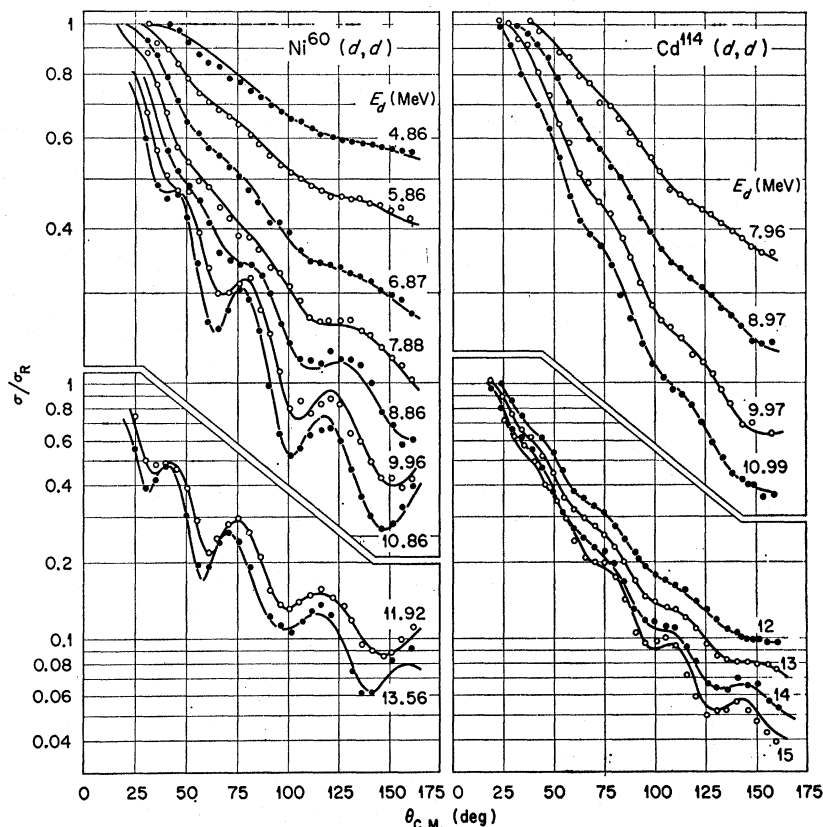


FIG. 1. Differential cross sections for deuterons elastically scattered from ^{60}Ni and ^{114}Cd . The solid curves represent optimum optical-model fits. The parameters for these fits are given in Fig. 4.

⁸ R. J. Silva and G. E. Gordon, Phys. Rev. **136**, B618 (1964).

⁹ These differential cross sections are reported in tabular form: J. K. Dickens and F. G. Perey, Oak Ridge National Laboratory Reports Nos. ORNL-3637, 1964 (unpublished) and ORNL-3727, 1965 (unpublished).

is defined by a real part

$$-V_S f(r, r_{0S}, a_S),$$

and by an imaginary part

$$4W_D a_I (d/dr) f(r, r_{0I}, a_I),$$

where $f(r, r_0, a)$ is the usual Woods-Saxon potential shape

$$f(r, r_0, a) = [1 + \exp((r - r_0 A^{1/3})/a)]^{-1},$$

and A is the atomic mass of the target nucleus.

A Coulomb potential due to a uniformly charged sphere of radius $r_{0C} A^{1/3}$ was included. Throughout this

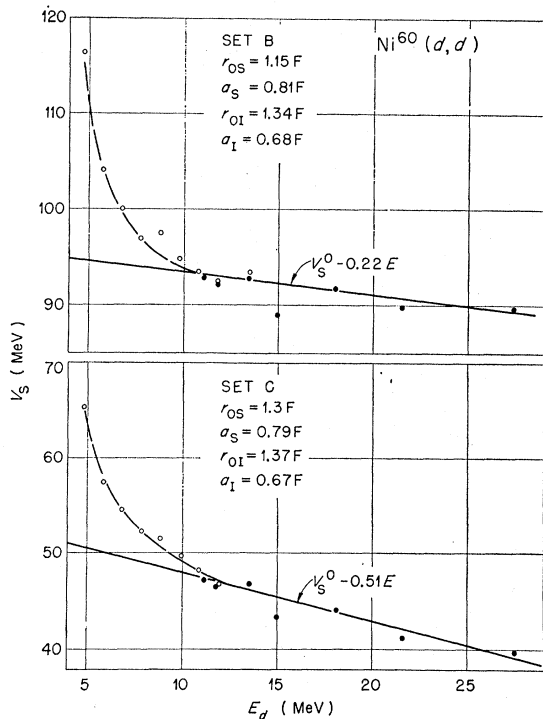


FIG. 2. Values of V_S obtained from the ^{60}Ni analysis with a standard optical model with no polarizability potential, for two sets of geometrical parameters. The solid lines indicate the linear behavior of V_S determined from analysis on higher energy data. The dashed curves are included to emphasize the low-energy behavior of V_S .

analysis, r_{0C} was set at 1.3 F. Although the particular choice of r_{0C} , within reasonable limits, does not affect the results at the higher energies, it is possible that at the lower energies the theoretical angular distributions are more sensitive to variations in r_{0C} . However, the energies considered are not much lower than Coulomb barrier, and the results of this analysis would not be significantly changed by a slightly different choice of r_{0C} .

The deuteron spin-orbit potential was neglected, since the calculated⁴ angular distributions are affected very little by this term at these energies.

The computer code used in this part of the analysis is a nonlinear least-squares search code, the same as that

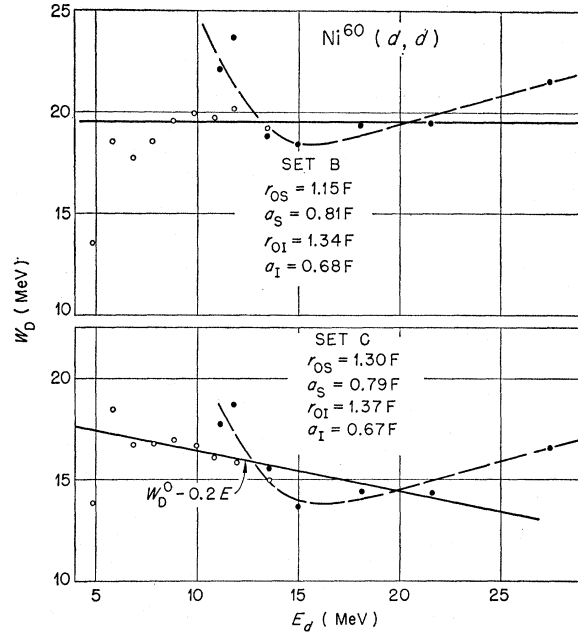


FIG. 3. Values of W_D obtained from the ^{60}Ni analysis using a standard optical model with no polarizability, for two sets of geometrical parameters. The solid lines indicate the behavior of W_D obtained in this analysis. The dashed lines indicate the trend observed in Ref. 1.

used previously.¹ The procedure in fitting the data consists in minimizing χ^2 , where

$$\chi^2 = \sum_i \left[\frac{\sigma_{\text{exp}}(\theta_i) - \sigma_{\text{th}}(\theta_i)}{\Delta\sigma_{\text{exp}}(\theta_i)} \right]^2,$$

by varying a certain number of parameters. An error of 5% was assigned to all data points, and the absolute cross sections were those determined experimentally. The preliminary analysis was done on the ^{60}Ni data, and then the procedure was applied to the ^{114}Cd data.

A. Standard Geometries

In Ref. 1, average sets of "geometrical parameters" (r_{0S}, a_S, r_{0I}, a_I) were used to analyze a large number of angular distributions by allowing only the well depths V_S and W_D to be adjusted to fit each individual angular distribution. In the present analysis, geometrical sets B (of Ref. 1) ($r_{0S}=1.15$ F, $a_S=0.81$ F, $r_{0I}=1.34$ F, $a_I=0.68$ F) and C ($r_{0S}=1.30$ F, $a_S=0.79$ F, $r_{0I}=1.37$ F, $a_I=0.67$ F), which are used with two different families of potentials differing essentially in the depths of the potential wells, were tried on the ^{60}Ni data. Very satisfactory fits to the data were obtained over the entire energy range. The values found for V_S and W_D are given in Figs. 2 and 3, together with the results of Ref. 1 for nickel at higher energies. Significant departure of V_S from the linear trend as a function of energy appears below 10 MeV. For the imaginary well depths W_D , the results of Ref. 1 (indicated by the dashed line on Fig. 3)

seem to show a very pronounced rise in this potential below 15 MeV; however, in the analysis of our data there is no evidence for such behavior. In the previous analysis¹ it had been concluded that this rise in W_D , which had been observed for several nuclei, was real. Now, however, this effect is not believed to be real, particularly when the effects of the absolute normalization of the data are considered.¹⁰ (The rise in W_D for 27.5 MeV¹ may have been due to the necessity of using a spin-orbit potential at this higher energy.⁴)

B. Best Geometries

An attempt was made to determine a particular set of geometrical parameters which would apply best to our present data. The data were fitted with the search code, with all six parameters allowed to vary. Large variations in the parameters were observed. An average value of r_{0S} of 1.18 F was obtained independently for both ⁶⁰Ni and ¹¹⁴Cd. Fixing r_{0S} at this value, the data were refitted by varying the other five parameters. Much less fluctuation in parameters resulted, compared with the previous case. The average values of the geometrical parameters obtained for ⁶⁰Ni were $r_{0S}=1.18$ F, $a_S=0.866\pm 0.034$ F, $r_{0I}=1.36\pm 0.03$ F, $a_I=0.682\pm 0.02$ F; and for ¹¹⁴Cd were $r_{0S}=1.18$ F, $a_S=0.866\pm 0.30$ F, $r_{0I}=1.30\pm 0.02$ F, $a_I=0.746\pm 0.050$ F.

The only definite difference in these two sets of parameters is in the value of r_{0I} . In view of the large effect due to errors in the normalization of the data, it is not known whether this difference is really significant or not, but it is required to fit this particular set of measured cross sections. The equality in a_S for both targets is

probably fortuitous in view of the fluctuations in parameters for both nuclei.

With the use of these two sets of parameters, all the data were fitted by varying only V_S and W_D . The fits are given in Fig. 1, and the parameters as a function of energy are shown in Fig. 4. The rapid rise of V_S below 10 MeV has not been improved by choosing a geometry suited to each nucleus for a better fit.

Many other variations of parameters were used in an effort to prevent the rise in V_S at low energies, but without success. If V_S is held fixed to the value determined by the linear extrapolation from higher energies, and r_{0S} is allowed to vary, then r_{0S} increases. If r_{0S} is fixed, and V_S is held to the value determined by the linear extrapolation, then a_S increases at lower energies. Of course, we cannot be sure that no combination of parameters r_{0S} and a_S exists that will prevent a rise in V_S at low energies, but we have not succeeded in finding one.

From an optical-model point of view there is no real objection to such a variation in parameters, since it is monotonic and smooth as a function of energy. Furthermore, this variation may be necessary to account for a particular reaction mechanism, which is important and has a large energy dependence below 10 MeV. Several mechanisms might explain this behavior. At low energies a few strongly coupled reaction channels might give rise to this large energy dependence. It is more likely that the real or virtual excitation of the deuteron by the electric field of the nucleus may increase in importance at these low energies. In the next section, we consider the effects of electric polarizability of the deuteron on the optical-model analysis.

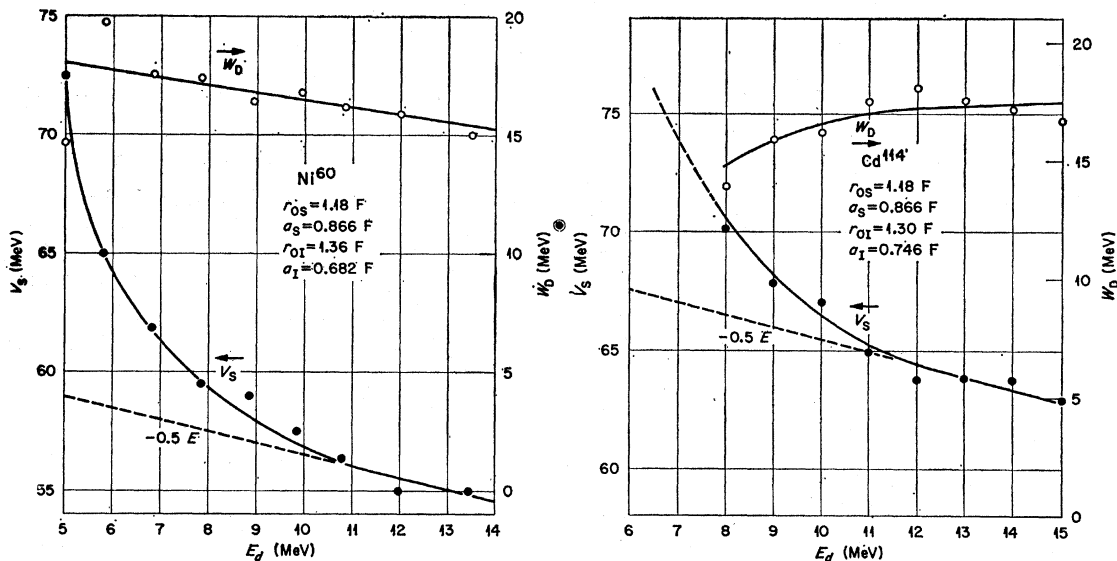


FIG. 4. Well depths obtained using the best geometry obtained for each nucleus in a standard optical model with no polarizability potential. The behavior of V_S at low energies is the same as that shown in Fig. 2.

¹⁰ J. K. Dickens and F. G. Perey, preceding paper, Phys. Rev. 138, B1080 (1965).

IV. THE OPTICAL MODEL WITH ELECTRIC POLARIZABILITY

The wave equation for the internal motion in a deuteron placed in a uniform electric field \mathbf{E} is

$$[-(\hbar^2/2M)\nabla_r^2 + V(r) - \frac{1}{2}e\mathbf{E}\cdot\mathbf{r}]\psi(r) = [\epsilon + \eta(E)]\psi(r),$$

where M is the nucleon mass, \mathbf{r} is the coordinate of relative motion, and ϵ is the deuteron binding energy. For an adiabatically applied electric field \mathbf{E} the electric polarizability α of the deuteron is defined by

$$\alpha = -2\eta(E)/E^2,$$

where η is of order E^2 .

Various calculations of α have been made by using different methods.¹¹⁻¹⁴ The results of these calculations are essentially in agreement and give for α a value of $\sim 0.5 \times 10^{-39}$ cm³.

To calculate the polarizability potential affecting the scattering of deuterons from nuclei, the charge of the deuteron is centered at the center of mass of the deuteron instead of at the proton coordinate, and the residual potential is expanded in multipoles. Keeping only the dipole term leads to the polarizability potential

$$-\frac{1}{2}[(Z^2 e^2 \alpha)/R^4],$$

where Z is the charge of the target nucleus, and R is the relative coordinate of the deuteron-nucleus system.

Several calculations of deuteron elastic scattering have been made in which only the Coulomb field and the electric polarizability were considered. The early calculations of Malenka *et al.*¹⁵ and of Sawicki¹² gave a very small departure from Coulomb scattering, of the order of a few percent. The recent calculation by Clement, however, gives an effect that is an order of magnitude larger.⁷ Using perturbation methods, Clement calculated the effect of the polarizability potential by taking the transition matrix elements between Coulomb waves. We have programmed in our optical-model code the above polarizability potential; by turning off the nuclear potential we should be able to reproduce Clement's calculations. With a $1/R^4$ potential, the range of integration has to be carried to a much larger radius than is normally done in optical-model calculations. Our results disagree with Clement's results by being about an order of magnitude smaller. We are, therefore, in agreement with the earlier calculations as to the magnitude of the effect. Bassel¹⁶ has recently incorporated the same polarizability potential in a different optical-model code and has obtained exact agreement with our calculations.

The effects of adding the polarizability potential, with a value of $\alpha = 0.5 \times 10^{-39}$ cm³, to the optical-model potential, found for best fits at three values of the deuteron energy, are shown in Fig. 5 for ¹¹⁴Cd. Calculations were also performed for nickel, but because of the lower Z the effects are smaller than they are for cadmium. The main change in the angular distributions is a rotation of the theoretical curve, with the cross section at 175° being increased by 6%. Although the effects of the polarizability are small, they are not entirely negligible, and the inclusion of this additional potential will modify the results of optical-model analyses, particularly at lower energies.

An attempt to fit the data for nickel and cadmium by using set *C* geometry but including the polarizability of the deuteron (with $\alpha = 0.5 \times 10^{-39}$ cm³) led to a slight reduction (~ 2 MeV) in the real-well depth V_s , and a slight increase (~ 2 MeV) in the imaginary-well depth W_D . Although the effects were in the right direction to decrease the rise in V_s at low energies, they did not

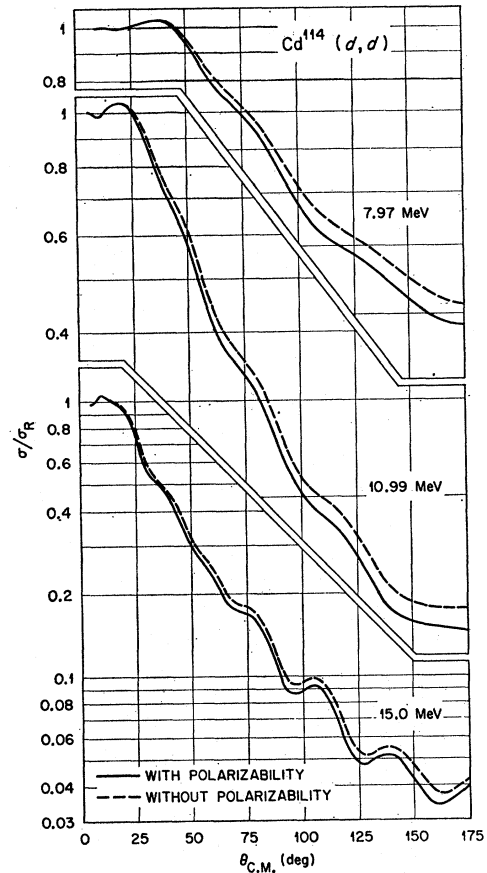


FIG. 5. Calculated angular distributions showing the effect of the inclusion of the polarizability potential. The dashed curves represent the best fits obtained to ¹¹⁴Cd data using the parameters shown in Fig. 4 in a standard optical model with no polarizability potential. The solid curves are the calculated angular distributions using the same sets of parameters and including the polarizability potential, with $\alpha = 0.5 \times 10^{-39}$ cm³.

¹¹ N. F. Ramsey, B. J. Malenka, and U. E. Kruse, Phys. Rev. **91**, 1162 (1953).

¹² J. Sawicki, Acta Phys. Polon. **13**, 225 (1954).

¹³ B. W. Downs, Phys. Rev. **98**, 194 (1955).

¹⁴ C. F. Clement, Phys. Rev. **128**, 2724 (1963).

¹⁵ B. J. Malenka, U. E. Kruse, and N. F. Ramsey, Phys. Rev. **91**, 1165 (1953).

¹⁶ R. H. Bassel (private communication).

eliminate it. Furthermore, the quality of the fits was not improved; instead, it was worsened at the highest energies. This is not surprising, since the set C geometry was determined without this additional potential.¹ Parameter searches on the five highest energies, with r_{0s} kept fixed at 1.18 F and α at 0.5×10^{-39} cm³, yielded different sets of geometrical parameters from those obtained in the previous section where α was zero.

We did not attempt a more extensive fitting of the data by using the polarizability potential, since we felt that incorporating virtual excitations of the deuteron without in some manner treating the electric breakup of the deuteron would be inconsistent. At present, there is no simple treatment of the electric breakup of the deuteron in a formalism which can be easily incorporated in an optical-model calculation. Possibly a long tail, which might simulate the deuteron breakup, could be added to the imaginary part of the optical potential. However, we feel that some theoretical justification should be given to the shape and strength of this imaginary potential, because the lack of structure in the angular distribution would certainly allow a wide range

of shapes and strengths on a purely phenomenological basis.

V. CONCLUSIONS

The data presented in this paper may show evidence for some effects of the nuclear electric field on the deuteron during elastic scattering from nuclei. Since the departure from Rutherford scattering is many times larger than that expected from the electric polarizability of the deuteron alone, we must conclude that nuclear interactions still dominate the elastic scattering even at the lowest energies of our measurements. The lack of structure of the deuteron elastic-scattering angular distributions at low energies is a very serious handicap to a phenomenological analysis of the data. We feel that more theoretical attention should be given to the electric breakup of the deuteron before any meaningful optical-model analysis of the data can be extended to low deuteron bombarding energies.

ACKNOWLEDGMENTS

We take great pleasure in acknowledging the valuable assistance of R. H. Bassel, G. R. Satchler, R. J. Silva, and G. F. Wells.

Some Energy Levels in P^{30} Observed in Radiative Capture by Si^{29} of Protons with Energies from 1420 to 2160 keV*

P. A. PHELPS,† E. A. MILNE, AND H. E. HANDLER
U. S. Naval Postgraduate School, Monterey, California
 (Received 28 January 1965)

The excitation function for the $Si^{29}(p,\gamma)P^{30}$ reaction has been experimentally determined in the proton energy range from 1420 through 2160 keV. Unreported resonances in this reaction have been identified at 1975, 2033, 2075, and 2117 keV with estimated errors of ± 4 keV, corresponding to energy levels in P^{30} at 7.49, 7.55, 7.59, and 7.63 MeV. Gamma spectra at these resonances are obscured by contaminant radiation but suggest complex decay schemes. Double angular-correlation measurements have been made at the 1470-keV resonance indicating a resonance-level spin of $2+$, or less probably, $2-$. The level at 4.50 MeV in P^{30} is shown to probably have a spin of $2+$ or, less probably, $3+$; these spin values are in disagreement with the $0+$ that has been predicted for this level.

I. INTRODUCTION

THE results of a study of the $Si^{29}(p,\gamma)P^{30}$ reaction, herein reported, consist of two parts. The first consists of observations of the excitation function between 1420 and 2170 keV and, in particular, of four resonances which have been found at the proton energies: 1975, 2033, 2075, and 2117 keV. The second reports on a double γ - γ angular-correlation experiment at the 1470-keV resonance.

Previous investigations of this reaction were summarized in the compilation of Endt and Van der Leun.¹

Recent investigators have been Baart *et al.*,² Moore,³ and Ejiri *et al.*⁴

II. EXPERIMENTAL PROCEDURE

The 2-MeV Van de Graaff accelerator at the U. S. Naval Postgraduate School was used to bombard isotopically enriched SiO_2 (91.8% Si^{29} ; 7.8% Si^{28} ; 0.30 Si^{30}) purchased from the Oak Ridge National Laboratory. Targets of $\frac{1}{2}$ 5- to 8-keV thickness for 2-MeV protons were produced by vacuum plating enough high-purity

* Research work supported in part by the U. S. Office of Naval Research.

† Present address: U. S. Naval Academy, Annapolis, Maryland.

¹ P. M. Endt and G. Van der Leun, Nucl. Phys. 34, 151 (1962).

² E. E. Baart *et al.*, Proc. Phys. Soc. (London) 79, 237 (1962).

³ R. A. Moore, Ph.D. thesis, University of Kansas, 1963 (unpublished).

⁴ H. Ejiri *et al.*, Nucl. Phys. 51, 470 (1964).